Upgrading SIM–OFDM Using a Threshold for Correct Operation with Analytical Proofs

Ahmed N. Jabbar, Samir J. Almuraab, and Abdulkareem A. Kadhim, Senior Member, *IEEE*

Original scientific article

***Abstract*—A new upgrade to the SIM–OFDM is suggested to solve a critical problem that crashes the system even over noiseless channel. This problem is the interference of the zeros at the IFFT output with the B_{OOK}'s zeros that confuses the receiver during demodulation which leads to BER accumulation. The suggested solution is to use a threshold to differentiate the data carried by the B_{OOK} from the IFFT's symbols. The new system is called Threshold SIM–OFDM (TSIM–OFDM). The mathematical analysis of TSIM–OFDM proves it operates normally and meets the theoretical bounds. The TSIM–OFDM preserves the probability of 1 equal to ½. This preservation comes from the direct connection of the ON/OFF switching bits to the subcarrier which overrides the majority condition. This new switching technique simplifies the system operation resulting in higher transmission speed and increased spectral and power efficiency. A simple approach to derive the BER for the SIM–OFDM is presented which proves that the SIM–OFDM will never reach zero BER level unlike the TSIM–OFDM. The simulation results show that the TSIM–OFDM BER reaches zero level and the output power is almost half of the OFDM. Adding the threshold will increase the transmitted power slightly and tends to decrease with the increase of IFFT length.**

***Index terms*—SIM–OFDM, multicarrier OFDM, low transmission power communication, green communication system, high spectral efficiency communication, low complexity SIM–OFDM.**

I. Introduction

The communication systems are playing a major role in the development and progress of modern societies. These communication systems orchestrate multiple life aspects like e–commerce, e–health, exchanging expertise among scholars, connecting people via social networks even managing military sensitive operations [1–10]. Hence, they face many challenges especially the data load that is increasing exponentially each year [11]. To handle such massive data loads, the communication systems should increase the transmission power and/or bandwidth.

The available spectrum for transmission has become scarce and valuable due to extensive usage. Also, the high–power and high–frequency transmission may create health hazards to those live near the base stations [12–15]. Therefore, new techniques in designing the communication systems are emerging to solve the power/bandwidth problems. These techniques are trying to distribute the power over multiple paths to reduce its intensity or increasing the transmitter directivity to maximize the received power [16–21]. The latest attempt in this field is the Index Modulation (IM). The IM was implemented with the OFDM subcarriers creating Subcarrier Index Modulation OFDM (SIM–OFDM) that appeared in 2009 [22]. The SIM–OFDM uses binary data frames called Bit ON OFF Keying (B_{OOK}) to switch the subcarriers OFF if B_{OOK} = 0 or ON when B_{OOK} = 1. The bits in the B_{OOK} are passed through a condition called majority condition N_{maj} to check the 1s repetition. If the 1s are qual or higher than the 0s then the B_{OOK} is passed to the subcarriers sections else the B_{OOK} bits are inverted before they are used for switching. This technique promised a –3 dB power reduction with spectral efficiency increment. The SIM–OFDM was implemented by many applications to improve the link quality and safety [23– 26]. Since its appearance, the SIM–OFDM passed through corrections to improve its performance [27–30]. The authors of [31] proved analytically that SIM–OFDM is incapable to satisfy its claims and cannot reach the – 3 dB power reduction. Also, they showed that the BER is complicated with multiple sources that leads to system instability.

The first contribution in this paper is highlighting, for the first–time, the zero–interference problem that will render the SIM–OFDM inoperable even over an ideal noiseless channel. This problem happens when the IFFT output contains 0s that will interfere with the B_{OOK} 0s leading to the receiver's confusion. This confusion will crash the system due to Bit Error Rate (BER) accumulation. This problem is fully illustrated and analyzed in this paper with examples of the sequences that will shut down the link. A simple solution is suggested for this problem by using a threshold that will bring the SIM–OFDM back to normal operation. This new system is referred to as Threshold SIM–OFDM (TSIM–OFDM). The threshold will separate the B_{OOK} 0s from the IFFT 0s and acts as an optimum detection threshold. The second contribution is the direct connection between the B_{OOK} and the subcarrier section to preserve the probability of 1, $p(1)$, to be always ½ to ensure the – 3 dB power reduction. This new arrangement simplifies the SIM–OFDM operation to increase its speed and improve its BER performance. The third contribution is the mathematical procedure suggested by this paper to derive the analytical equation for the BER for any SIM–OFDM based system to assess its operation. This procedure proves

Manuscript received September 11, 2023; revised October 13, 2023. Date of publication November 9, 2023. Date of current version November 9, 2023. The associate editor prof. Gordan Šišul has been coordinating the review of this manuscript and approved it for publication.

A. N. Jabbar and S. J. Al-Muraab are with the Department of Electrical Engineering, University of Babylon, Iraq (e-mails: Ahmed_AlJafari@yahoo.com, Dr.samiralmuraab@uobabylon.edu.iq).

A. A. Kadhim is with the Computer Techniques Engineering Department, Al-Mustaqbal University, Iraq (e-mail: ak.kadhim@uomus.edu.iq).

Digital Object Identifier (DOI): 10.24138/jcomss-2023-0131

undoubtedly that the original SIM–OFDM BER [22] will not converge to 0 even over noiseless channel. The new TSIM–OFDM performance is verified using simulation and mathematical derivations to prove its successful operation.

Section II presents the zero–interference problem, its causes and the TSIM–OFDM structure and operation. Section III gives the TSIM–OFDM performance evaluation regarding Spectral Efficiency (SE), transmission rate and the BER analysis. Section IV contains the simulation results to provide the proof that the TSIM–OFDM operates successfully. Section V contains the final conclusions.

II. The TSIM–OFDM Concepts and Operation

This section explains the problem of the zeros generated by the IFFT, how do they interfere with the B_{OOK}, the threshold effect and the TSIM–OFDM structure and operation.

A. Sequence Types that Generate 0(s) at the IFFT Output

The IFFT is a linear operator that transforms the frequency samples to time domain. The IFFT twiddles are symmetrically allocated around the unit circuit as equal positive/negative values. This allocation is the main reason for the 0s generated at the IFFT output because they can null each other when added [32]. Assume an IFFT length N connected to QAM mappers containing 2^M symbols where M is the bits/symbol then the number of IFFT input states are $2^{M \times N}$. The probability of selecting any state is $2^{-N \times M}$ [33]. If the selected state contains N Repeated Number Sequence (RNS), the IFFT output will contain N zeros if all the numbers are 0 or $N-1$ if the numbers are not equal to zero. If the chosen state consists of Subsets with Evenly Repeated Number (SERN) then the IFFT output will contain a single 0 located at $N/2–1$ of the output. The most difficult sequence is when N is divided into Repeated Subset with the Same Number Sequence (RSSNS), then the output will contain different number of 0s at different locations depending on the subset's contents. These sequences for $N = 16$ are illustrated in Fig. 1 for clarity

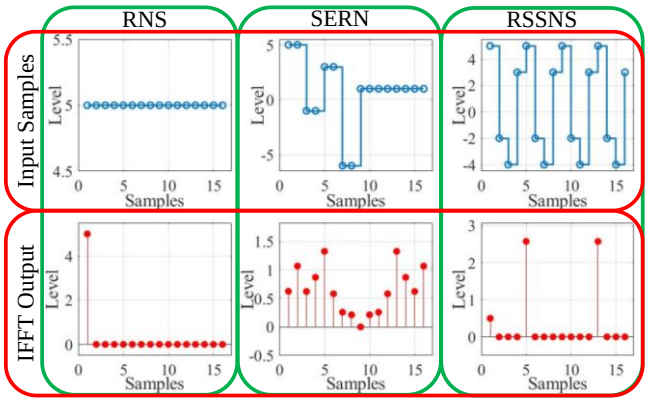

Fig. 1. Sequences generating 0 at the IFFT output

To understand why the 0s at the IFFT's output crash the SIM–OFDM system, the SIM–OFDM principles of operation must be revisited. The SIM–OFDM assumes when the $B_{OOK} = 0$, the carrier at this index is turned off and no data are transmitted. This state is called a forbidden state (×). If the $B_{OOK} = 1$ then the subcarrier is activated to modulate the IFFT data [22]. Hence, the functionality of the SIM–OFDM can be summarized as in Table I where S is the IFFT output symbol's value.

TABLE I
THE B_{OOK} AND IFFT INTERACTION FOR SIM–OFDM

TRANSMITTER	IFFT	×	$S = 0$	$S \neq 0$
	B_{OOK}	0	1	1
RECEIVER	R_x	0	0	S

Table I shows that when the received symbol $R_x = 0$, then the receiver cannot decide whether the symbol $S = 0$ or the $B_{OOK} = 0$, as highlighted in red in Table I, and that will definitely crash the system. To avoid this confusion, a threshold value (γ) can be used to enable the receiver to differentiate that the 0 either belongs to IFFT or B_{OOK}. Adding a γ to the IFFT output transforms the SIM–OFDM operation from Table I to Table II.

TABLE II
THE B_{OOK} AND IFFT INTERACTION FOR SIM–OFDM WITH γ

TRANSMITTER	IFFT	×	$S = \gamma$	$S + \gamma \neq 0$
	B_{OOK}	0	1	1
RECEIVER	R_x	0	γ	$S + \gamma$

Table II shows that R_x takes tristate values which are 0, γ and $S + \gamma$. Each state is now related to a unique B_{OOK}/IFFT combination which resolves the confusion problem. After separating the B_{OOK} from the IFFT, the γ can be removed at the receiver to recover the original IFFT symbols. This threshold approach is implemented with the SIM–OFDM creating the TSIM–OFDM. The effect on the IFFT's output symbols before and after adding γ is shown in Fig. 2.*a* and Fig. 2.*b* respectively for $N = 16$

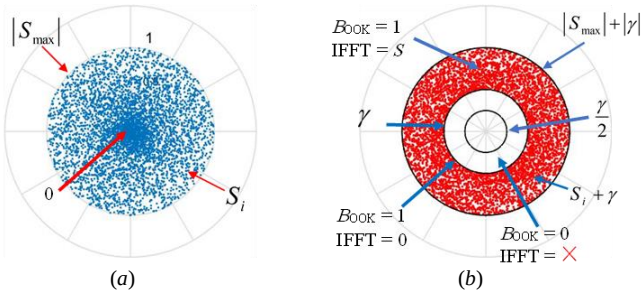

Fig. 2. The threshold addition effect on the IFFT output, (*a*) without threshold, (*b*) after adding the threshold

It is clear from Fig. 2.*a* that the IFFT's output is densely packed at the origin which creates the confusion at the receiver as shown by Table I. However, after adding γ, the origin and the area around are cleared for the forbidden state only as shown by Fig. 2.*b*. Table II states are indicated on Fig. 2.*b*.

B. The TSIM–OFDM System Operation Concepts

The main problem facing the SIM–OFDM is the presence of the N_{maj} that alters and deforms the $p(1)$ resulting in less spectrum and energy efficiency. Also, N_{maj} disturbs the BER

resulting in system's instability [31]. Therefore, this stage should be removed to ensure proper operation. The removal is achieved by setting the number of QAM mappers equals to N in TSIM–OFDM rather than $N/2$ in SIM–OFDM [22] to connect the B_{OOK} directly to the subcarriers section.

In the beginning, the incoming data are converted to bits using any binary representation system. The well–known Fixed Point Number (FPN) representation is used to convert the data to binary system. The FPN represents the data using a fixed bits length F that is divided into two parts which are the integer part and fraction part. After converting the data to bits using FPN, these bits are divided into two blocks which are the B_{OOK} block that contains $F \times N$ bits and data repository block stacked as M rows as shown in Fig. 3.

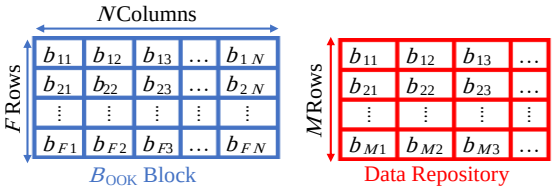

Fig. 3. Dividing FPN data into B_{OOK} binary block and data repository feeding the QAM mappers.

The B_{OOK} block switches the subcarriers ON/OFF while the data repository is fed to the QAM mappers and then to the IFFT stage. The block diagram of the TSIM–OFDM is shown in Fig. 4. that illustrates how the B_{OOK} block's bits are directly fed to the subcarrier section and the transmitted subcarriers pattern. The TSIM–OFDM draws a row from the B_{OOK} block and draws columns from the data repository equal to the number of 1s in this B_{OOK} row.

These columns are fed to the QAM mappers and then to the IFFT. The output of the IFFT is divided into real and imaginary and checked for the sign. If the real or the imaginary equals or higher than 0 then + γ is added otherwise – γ is added. Then after, these real and imaginary are combined before modulation using the active subcarriers.

After receiving the transmitted symbols, the detector will compare their energy to the optimum threshold $|\gamma|/2$ as shown Fig. (2.*b*). If the received symbol is below $|\gamma|/2$, then a 0 is placed in the B_{OOK} at the same index without any QAM demodulation. If the symbol equals or higher than $|\gamma|/2$ then a 1 is placed in the B_{OOK} and the symbol is decoded by the QAM after removing γ. When the B_{OOK} block in the transmitter is completed, another block is generated from the remaining data in the repository to start the transmission cycle. At the receiver, when F rows of the B_{OOK} are received, the B_{OOK} is combined with the QAM demodulated symbols to retrieve the original data. Obviously, the operation of the TSM–OFDM is much simpler than the SIM–OFDM also there is no need to synchronize the transmitter and receiver as needed by the SIM–OFDM [22-31]. This simplicity increases the transmission speed and decreases the BER level due to the elimination of the N_{maj}. The bits arrangement in Fig. 3. is not compulsory and can be rearranged in any possible way that fits the designers' preferences.

III. The TSIM–OFDM Performance Analysis

This section presents the mathematical analyses that describe the TSIM–OFDM performance like the SE, the transmission rate, transmission ratio and the BER. The BER analysis followed here is very simple and easy to be applied to any modified SIM–OFDM system. It proves, undoubtedly, that the SIM–OFDM in [22] cannot work properly.

A. The Spectral Efficiency, Transmission Rate and Ratio of the TSIM–OFDM

The TSIM–OFDM is upgraded to preserve the $p(1) = ½$ as discussed above. Hence, the transmission rate for the TSIM–OFDM is given by **Error! Reference source not found.**

$$R_{TSIM} = p(1) \times M \times N + N = N\left(\frac{M}{2} + 1\right) \qquad (1)$$

while the transmission rate of the OFDM (R_{OFDM}) is $M \times N$ which leads to the Transmission Ratio (T_R) of the TSIM–OFDM as shown in (2)

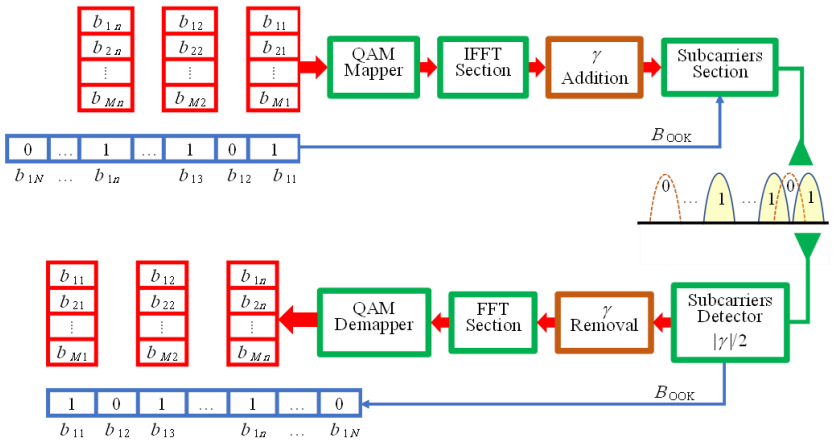

Fig. 4. The TSIM–OFDM transmitter receiver block diagra

$$T_R = \frac{R_{\text{TSIM}}}{R_{\text{OFDM}}} = \frac{N\left(1+\frac{M}{2}\right)}{M \times N} = \frac{1}{2}+\frac{1}{M}. \quad (2)$$

The T_R for the TSIM–OFDM reached the theoretical value suggested by [22] which exceeds the OFDM for the Binary PSK (BPSK) system, equivalent to the OFDM for the Quaternary PSK (QPSK). However, when M start to increase, T_R approaches ½ level.

The spectral efficiency (η) is defined as the amount of data carried per carrier. Thus, η for TSIM–OFDM can be calculated as in (3) [34, 35] where the average active carriers are N_a = ½ because $p(1)$ is preserved at ½

$$\eta_{\text{TSIM}} = \frac{N_a \times M}{N} + \frac{\left\lfloor \log_2\left(C_N^{N-N_a}\right)\right\rfloor}{N} = \frac{M}{2}+1 \quad \text{bit/s/Hz} \quad (3)$$

where $C_N^{N-N_a}$ is the combination function and $\lfloor\cdot\rfloor$ is the floor function. This maximum theoretical level of η can be reached only when $p(1)$ = ½ which is achieved by TSIM–OFDM.

B. The Bit Error Rate Analytical Derivation and Analysis

The BER occurs when the noise interacts with the symbol's power deviating it from its correct value. Looking back to Table II, it can be seen that the TSIM–OFDM is a tristate system with output powers 0, E_γ and E_{IFFT}^{γ} correspond to 0, γ and $S + \gamma$ symbol levels respectively. Hence, these power level will be the mean of the Additive White Gaussian Noise (AWGN) as shown in Fig. (5)

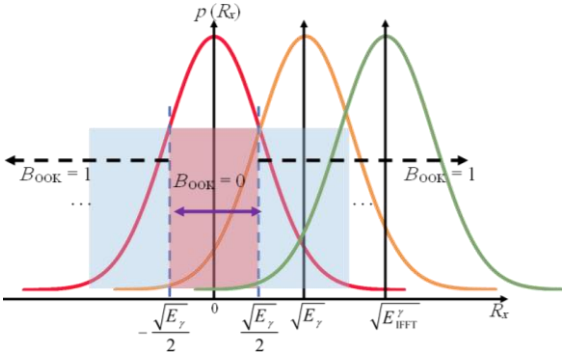

Fig. 5. The AWGN distribution in TSIM–OFDM

The optimum threshold in Fig. (5), as depicted in Fig. (3.*b*), is $\left|\sqrt{E_\gamma}\right|/2$. The TSIM–OFDM has two paths for data transmission which are the B_{OOK} and the QAM. Starting with the B_{OOK} which contains a single bit takes either 0 or 1 value, then the B_{OOK} probability of error is given by (4)

$$P_e^{B_{\text{OOK}}} = p(0)\cdot P_e(0) + p(1)\cdot P_e(1) = \frac{1}{2}\left[P_e(0)+P_e(1)\right] \quad (4)$$

where $P_e(0)$ and $P_e(1)$ are the probabilities of 0 and 1 false detection respectively. The $P_e(0)$ occurs when the received power level of 0 symbol is higher than $\left|\sqrt{E_\gamma}\right|/2$ then $P_e(0)$ can be evaluated as given by (5), see Fig. (5)

$$P_e(0) = \frac{2}{\sqrt{\pi N_0}}\left[\int_{\frac{\sqrt{E_\gamma}}{2}}^{\infty} \exp\left(-\frac{x^2}{N_0}\right)dx\right] = 2Q\left(\sqrt{\frac{E_\gamma}{2N_0}}\right) \quad (5)$$

The $P_e(1)$ occurs when the symbol with level $\sqrt{E_\gamma}$ or $\sqrt{E_{\text{IFFT}}^{\gamma}}$ is less than $\left|\sqrt{E_\gamma}\right|/2$ or falls into the red region in Fig. (5). Hence, $P_e(1)$ can be evaluated as given by (6)

$$\begin{aligned} P_e(1) = \frac{1}{\sqrt{\pi N_0}}&\left[\int_{-\frac{\sqrt{E_\gamma}}{2}}^{\frac{\sqrt{E_\gamma}}{2}} \exp\left(-\frac{\left(x-\sqrt{E_\gamma}\right)^2}{N_0}\right)dx\right. \\ &\left.+\int_{-\frac{\sqrt{E_\gamma}}{2}}^{\frac{\sqrt{E_\gamma}}{2}} \exp\left(-\frac{\left(x-\sqrt{E_{\text{IFFT}}^{\gamma}}\right)^2}{N_0}\right)dx\right] \\ =& Q\left(\sqrt{\frac{E_\gamma}{2N_0}}\right)-Q\left(3\sqrt{\frac{E_\gamma}{2N_0}}\right) \\ &+Q\left(\frac{2\sqrt{E_{\text{IFFT}}^{\gamma}}-\sqrt{E_\gamma}}{\sqrt{2N_0}}\right)-Q\left(\frac{2\sqrt{E_{\text{IFFT}}^{\gamma}}+\sqrt{E_\gamma}}{\sqrt{2N_0}}\right) \end{aligned} \quad (6)$$

The other source of error is the QAM data path. The SER of the QAM, P_e^{QAM}, is given by (7) [36, 37 and 38]

$$\begin{aligned} P_e^{\text{QAM}} = 4\cdot Q&\left(\alpha\sqrt{\frac{E_S^{\text{Q}}}{2N_0}}\right)\left[1-\frac{1}{\sqrt{2^M}}\right. \\ &\left.-\left(1-\frac{2}{\sqrt{2^M}}+\frac{1}{2^M}\right)Q\left(\alpha\sqrt{\frac{E_S^{\text{Q}}}{2N_0}}\right)\right] \end{aligned} \quad (7)$$

where E_S^{Q} is the QAM average symbol's energy and $\alpha = \sqrt{3/\left[2\left(2^M-1\right)\right]}$ is the normalizing factor. Another error in the QAM path appears when B_{OOK} is falsely detected. When B_{OOK} = 1 and detected as 0 then a QAM symbol is removed from the data or when B_{OOK} = 0 is detected as 1 then an erroneous symbol is added. These false symbols are related to the probability of 1 and 0 respectively.

To evaluate the average QAM path BER, assume a process ψ containing K independent subprocesses and each process generates its own error e_i then the average probability error of ψ is given by (8) [33]

$$P_e(\psi) = \sum_{i=1}^{K} e_i \Big/ K \quad (8)$$

Hence, the total QAM probability of error ($P_e^{\text{T-QAM}}$) is given by (9) according to (8).

$$\begin{aligned} P_e^{\text{T-QAM}} &= \frac{1}{2}\cdot\left[P_e^{\text{QAM}} + p(1)\cdot P_e(1) + p(0)\cdot P_e(0)\right] \\ &= \frac{1}{2}\left(P_e^{\text{QAM}} + P_e^{B_{\text{OOK}}}\right) \end{aligned} \quad (9)$$

The TSIM–OFDM contains two error generating processes that are the B_{OOK}, and QAM. Thus, the TSIM–OFDM's average probability of error is given by (10) according to (8)

$$P_e^{\text{TSIM}} = \frac{1}{2}\left[P_e^{B_{OOK}} + P_e^{\text{T-QAM}}\right] \tag{10}$$

Substituting (4) and (9) in (10) yields (11)

$$P_e^{\text{TSIM}} = \frac{1}{4}P_e^{\text{QAM}} + \frac{3}{8}P_e(0) + \frac{3}{8}P_e(1) \tag{11}$$

The $P_e(0)$ and $P_e(1)$ are mutually exclusive random processes and both cannot occur simultaneously. The final result in (11) shows how simple this approach to evaluate the probability of error of SIM–OFDM, TSIM–OFM and any system derived from them. The key value in (11) is the probability of 1 and 0 that should be kept at ½ to minimize the BER. To prove that the SIM–OFDM is not working and its BER will not converge to 0 at all, then (5) and (6) are substituted in (11) which yields (12)

$$\begin{aligned} P_e^{\text{TSIM}} = {} & \frac{1}{4}P_e^{\text{QAM}} + \frac{3}{8}\left[2Q\left(\sqrt{\frac{E_\gamma}{2N_0}}\right)\right] \\ & + \frac{3}{8}\left[Q\left(\sqrt{\frac{E_\gamma}{2N_0}}\right) - Q\left(3\sqrt{\frac{E_\gamma}{2N_0}}\right)\right. \\ & \left. + Q\left(\frac{2\sqrt{E_{\text{IFFT}}^{\gamma}} - \sqrt{E_\gamma}}{\sqrt{2N_0}}\right) - Q\left(\frac{2\sqrt{E_{\text{IFFT}}^{\gamma}} + \sqrt{E_\gamma}}{\sqrt{2N_0}}\right)\right] \end{aligned} \tag{12}$$

When Setting $\gamma = 0 \Rightarrow E_\gamma = 0$ in (12), the TSIM–OFDM will be identical to SIM–OFDM and (12) will be as in (13)

$$P_e^{\text{TSIM}} = \frac{1}{4}P_e^{\text{QAM}} + \boxed{\frac{3}{8}}. \tag{13}$$

The SIM–OFDM in (13) shows that even over a noiseless channel or $P_e^{\text{QAM}} = 0$, the SIM–OFDM's probability of error will not converge 0 but to a constant value which is ⅜. This proof confirms the claims by this paper and the illustrations in Table I and Fig. 2.*a*. Thus, γ is mandatory for proper operation. However, setting γ to the optimum value for minimum BER is not an easy task because γ is related to IFFT average output symbol's power E_{IFFT}^{γ} which depends on N and E_S^{Q}. If γ is much higher than E_{IFFT}^{γ}, (13) will also converge to constant ⅜ and BER will not converge to 0. This can be verified by assuming $\gamma \to \infty \Rightarrow E_\gamma = \infty$ in (12). The experimental approach is followed to set optimum γ value using trial and error.

IV. The Simulation Settings and Results for the TSIM–OFDM

The TSIM–OFDM parameters $p(1)$, the output power and the BER are evaluated using simulation to show how the E_S^{Q} and N are affecting the system's performance and optimum γ. The tests are performed by sending 10^6 bits through an AWGN channel. In the first test, QAM is set to 64 symbols, M = 6, and γ is optimized experimentally. The IFFT length is changed to 128, 1024, 4069 and 16384 to test the N effect on the performance and the optimum γ. The transmitter and receiver flowcharts are shown in Fig. 6.*a* and Fig. 6.*b* respectively.

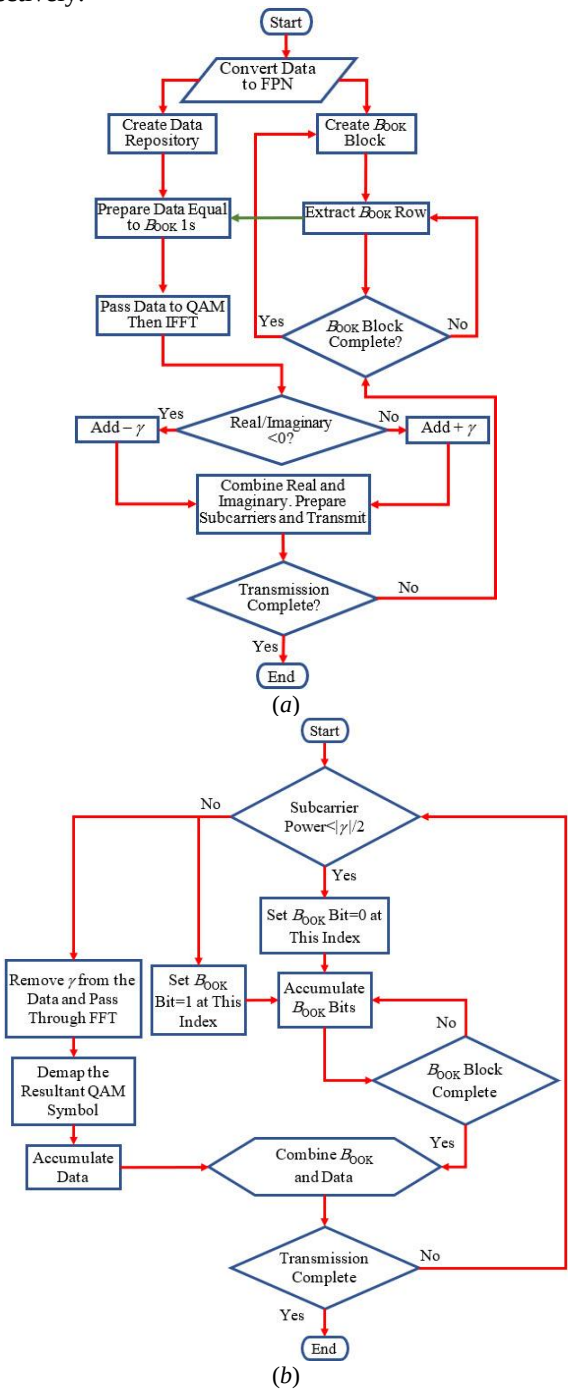

Fig. 6. The flowchart of the TSIM–OFDM: (*a*) The Transmitter, (*b*) The Receiver

The results for $p(1)$ are shown in Fig. 7. The $p(1)$ is measured instantaneously per frame (Inst. $p(1)$), the blue line, and as an average (Av. $p(1)$), the red line. It is clear that average $p(1)$ = ½ for all IFFT lengths even for a short sample as shown in Fig. 7.*d*. This preservation of $p(1)$ is very crucial

to ensure proper TSIM–OFDM performance with maximum efficiency as discussed in Section III.

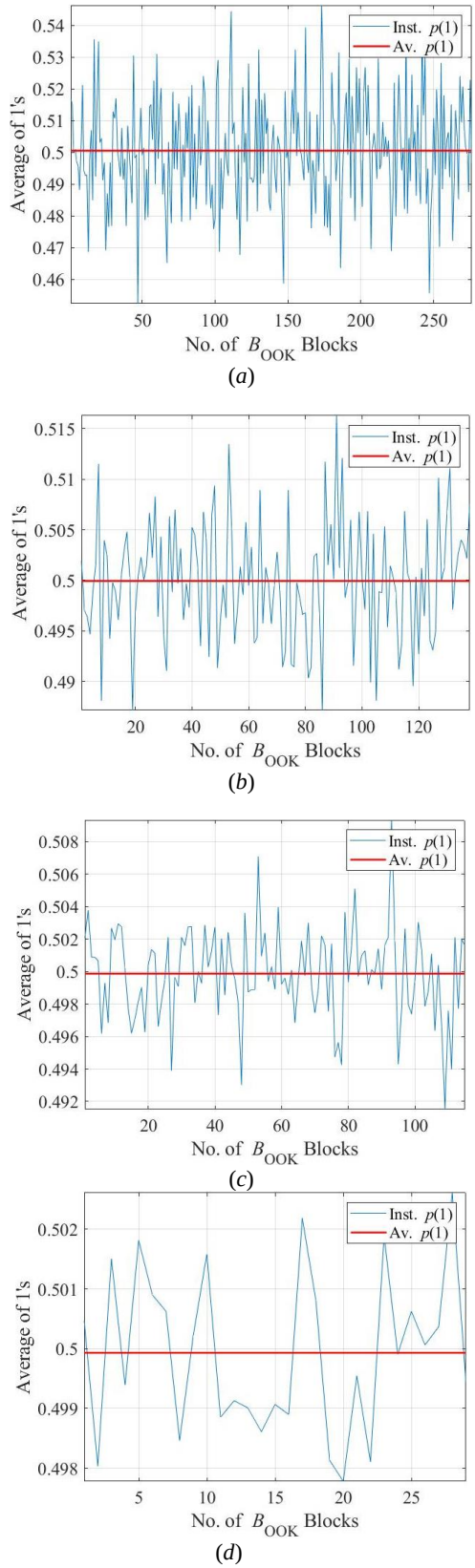

Fig. 7. The $p(1)$ results for M = 6 TSIM–OFDM system, (*a*) N=128, (*b*) N=1024, (*c*) N=4096, (*d*) N=16384

The output power test results are shown in Fig. 8. as an average per frame, blue line, and total average power, red line. The output power is equal between OFDM and TSIM–OFDM as these systems are power preservative. But, the number of frames in the TSIM–OFDM is twice the number of frames in the OFDM as shown in Fig. 8.

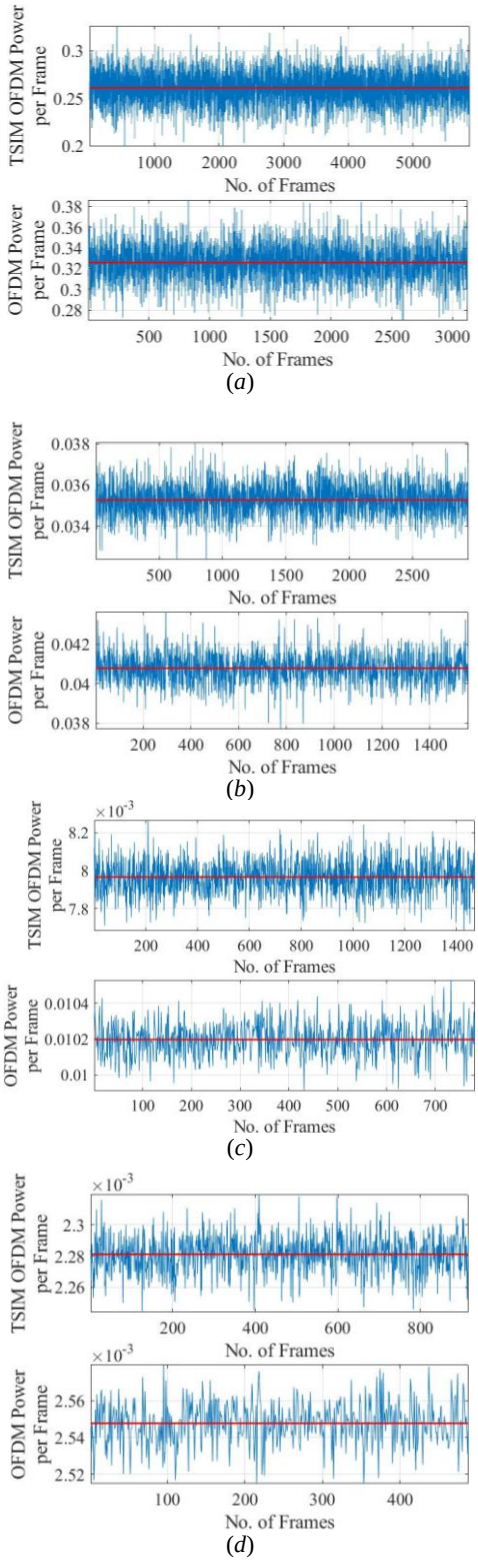

Fig. 8. The output power results for M = 6 TSIM–OFDM system, (*a*) N=128, (*b*) N=1024, (*c*) N=4096, (*d*) N=16384

When dividing the power by the number of frames, it can be seen that the TSIM–OFDM is working near – 3 dB power. The number of frames and power reduction level are summarized in Table III.

TABLE III
THE NUMBER OF OFDM AND TSIM–OFDM FRAMES AND REDUCTION LEVEL SUMMERY

N	OFDM FRAMES	TSIM–OFDM FRAMES	FRAMES RATIO	POWER REDUCTION (dB)
128	3125	5878	0.53	– 2.74
1024	1562	2942	0.53	– 2.74
4096	781	1470	0.53	– 2.74
16384	488	917	0.53	– 2.74

However, careful inspection for the average output power, red line, it can be seen that the TSIM–OFDM total average power is slightly above OFDM's half total average power. This increase in power comes from the added γ which increases the TSIM–OFDM's average frame's power. A summary of the γ effect on the TSIM–OFDM's Frame Average Power (F_{AP}) is given in Table IV.

TABLE IV
THE γ EFFECT ON THE TSIM–OFDM AVERAGE OUTPUT POWER SUMMARY

N	OFDM F_{AP}	TSIM–OFDM F_{AP}	γ POWER
128	0.326	0.2611	98.05×10^{-3}
1024	40.785×10^{-3}	35.264×10^{-3}	14.872×10^{-3}
4096	10.196×10^{-3}	7.966×10^{-3}	2.868×10^{-3}
16384	2.548×10^{-3}	2.281×10^{-3}	1.007×10^{-3}

The γ power can be calculated by subtracting TSIM–OFDM F_{AP} from half OFDM F_{AP}. The γ power is low and decreasing with N increase.

The results shown in Fig. 9. are for the BER test with optimized γ for minimum BER. The BER for the TSIM–OFDM is mainly dominated by the QAM BER because the number of the QAM symbol's bit is much higher than B_{OOK}'s. with higher weight in (11). However, examining the BER it can be seen that the QAM BER rapidly drops to 0 when B_{OOK} drops to 0 which verifies the assumptions for (9). The optimum γ used for the IFFT lengths is given by Table V.

TABLE V
THE OPTIMUM γ VALUES FOR MINIMUM BER SUMMERY

N	γ VALUE
128	0.18
1024	0.075
4096	0.03
16384	0.0205

Table V shows that the optimum γ value varies with N variation. However, the level is decreasing with N increasing leading to γ power decrement as given by Table IV. Overall, the BER results show that the TSM–OFDM is working properly with its BER is converging to 0.

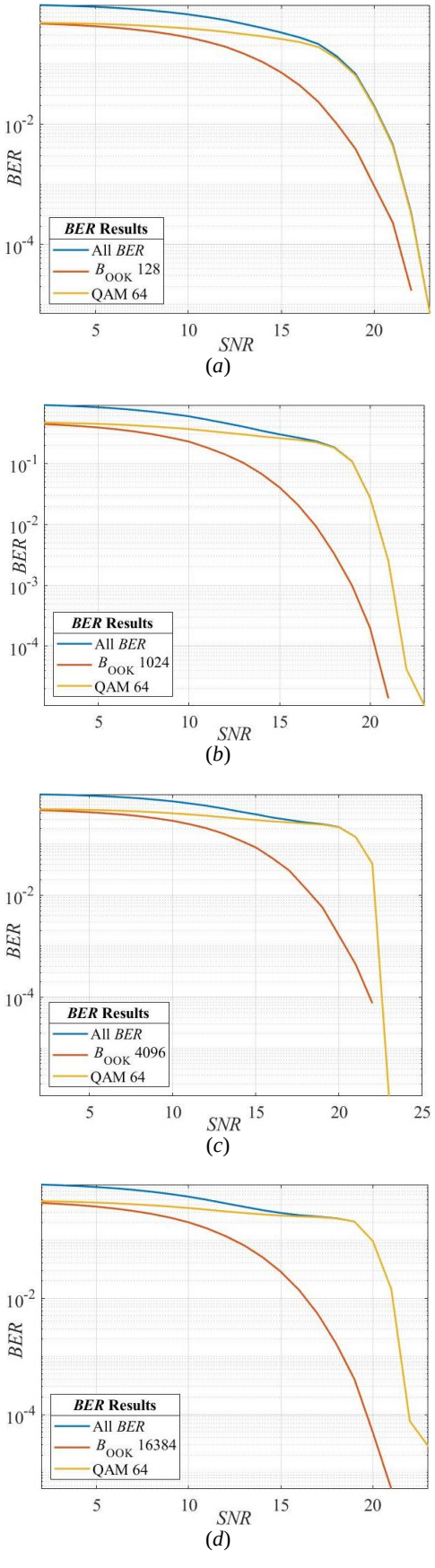

Fig. 9. The BER results for M = 6 TSIM–OFDM system, (*a*) N=128, (*b*) N=1024, (*c*) N=4096, (*d*) N=16384

The next parameter under investigation is E_S^Q that can be altered when 64 symbol levels QAM is replaced by 128 QAM symbol levels, M = 7. This new QAM alters the IFFT output symbol's level S by altering E_S^Q. The BER results using the same γ values in Table (V) are shown in Fig. (10). The QAM 128 levels BER results show that even when γ is not optimized for the new settings, the TSIM–OFDM BER still converges to zero. The effect of the non–optimized γ is clear on the B_{OOK} BER that is shifted to a higher Signal to Noise Ratio (SNR) causing QAM BER to increase.

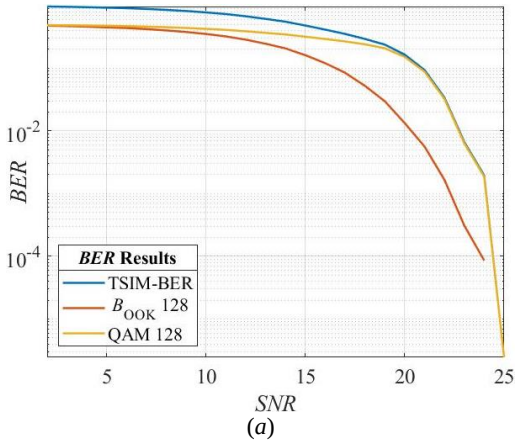

(*a*)

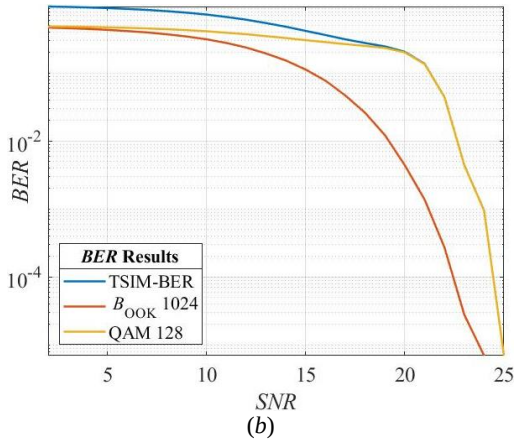

(*b*)

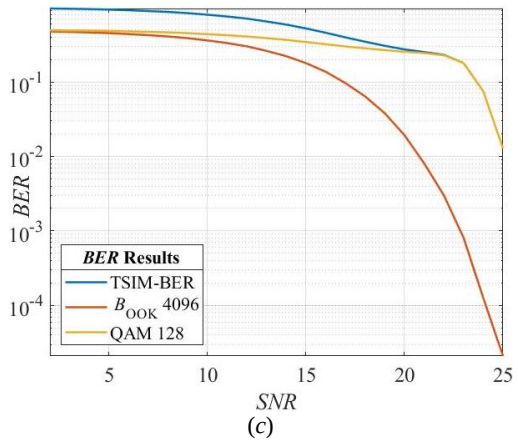

(*c*)

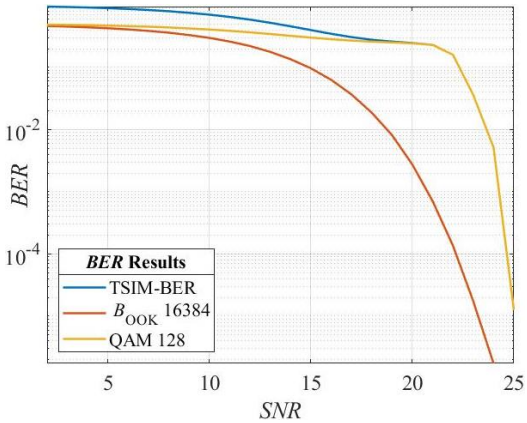

(*d*)

Fig. 10. The BER results for M = 7 TSIM–OFDM system, (*a*) N=128, (*b*) N=1024, (*c*) N=4096, (*d*) N=16384

Optimizing γ will give a better TSIM–OFDM BER performance. The BER results for QAM 128 levels show how important is γ for the SIM–OFDM system and without it the system fails to deliver the data even over noise free link.

V. Concluding Remarks

The TSIM–OFDM system preserves the $p(1)$ = ½ to achieve maximum system's efficiency. The TSIM–OFDM is simpler that SIM–OFDM due to the direct link between the B_{OOK} and the subcarrier section.

The SIM–OFDM and its derivatives suffer from the IFFT's 0s. These 0s interfere with the B_{OOK}'s 0s causing confusion at the receiver that leads to accumulated BER even over noiseless channel. A solution suggested by this research is by adding a threshold to the IFFT output to ensure the IFFT will not generate 0s. However, the threshold will slightly increase the TSIM–OFDM output power leading to power reduction decrement. Nevertheless, γ level decreases with the increase of N leading to higher power reduction. The γ provides the optimum detector boundaries unlike SIM–OFDM which are missing. The optimum value for γ cannot be easily calculated due to the interaction between IFFT and QAM. The experimental approach is followed by this research to evaluate optimum γ level. More accurate methods can be used like, optimization algorithms or artificial intelligence.

The TSIM–OFDM transmitted frames are twice the OFDM's. Thus, TSIM–OFDM average frame's power is half the OFDM average frame's power. This explains why the $p(1)$ should be kept to ½ to achieve the – 3 dB power reduction.

The TSIM–BER is dominated by the QAM because its symbol's bits are higher than the B_{OOK} with higher probability of error weight. However, the QAM is influenced by the B_{OOK} BER; thus, QAM BER drops to 0 when B_{OOK} is correctly detected. Equation (11) shows that the TSIM–OFDM QAM BER can reach ¼ the OFDM's BER if the B_{OOK} is correctly detected which represents a major reduction.

The simplified approach suggested by this research to derive the BER can be applied to any similar SIM–OFDM systems. This approach showed that the SIM–OFDM will not operate correctly unless a threshold is used.

The TSIM–OFDM can be said as the first correctly operational SIM–OFDM system and proved analytically and through simulation.

REFERENCES

[1] S. Deng *et al*., "Construction and Applications of Billion-Scale Pre-Trained Multimodal Business Knowledge Graph", *IEEE 39th International Conference on Data Engineering (ICDE)*, Anaheim, CA, USA, 2023, pp. 2988–3002.

[2] J. Gong *et al*., "Attention Weighted Mixture of Experts with Contrastive Learning for Personalized Ranking in E-commerce", *IEEE 39th International Conference on Data Engineering (ICDE)*, Anaheim, CA, USA, 2023, pp. 3222–3234.

[3] Z. Li and L. E. Calvet, "Extraction of ECG features with spiking neurons for decreased power consumption in embedded devices", *19th International Conference on Synthesis, Modeling, Analysis and Simulation Methods and Applications to Circuit Design (SMACD)*, Funchal, Portugal, 2023, pp. 1–4.

[4] Wen *et al*., "Noncontact Monitoring of Infant Apnea for Hypoxia Prevention Using a K-band Biomedical Radar", *IEEE/MTT-S International Microwave Symposium - IMS 2023*, San Diego, CA, USA, 2023, pp. 983–986.

[5] C. Huang, S. Ke and X. Liu, "Duopoly Business Competition in Cross-Silo Federated Learning" *in IEEE Transactions on Network Science and Engineering*, 2023.

[6] R. N. Wambua, "Systematic Review of the Influence of Internet of Things (IoT) on the Education of Students with Disabilities", *IST-Africa Conference (IST-Africa)*, Tshwane, South Africa, 2023, pp. 1–8.

[7] M. T. Nuseir *et al*., "The Role of Social Media Usage, E-WOM, and Perceived Enjoyment in Shaping Customer Attitudes and Blockchain Adoption Loyalty in UAE Banking: A Quantitative Investigation", *International Conference on Intelligent Computing, Communication, Networking and Services (ICCNS)*, Valencia, Spain, 2023, pp. 141–148.

[8] Y. Liu *et al*., "Evaluating Digital Health Services Quality via Social Media", *IEEE Transactions on Engineering Management*, 2023, (early Access).

[9] M. Y. M. Haq *et al*., "Assessing Network Operator Actions to Enhance Digital Sovereignty and Strengthen Network Resilience: A Longitudinal Analysis during the Russia-Ukraine Conflict", *IEEE European Symposium on Security and Privacy Workshops (EuroS&PW)*, Delft, Netherlands, 2023, pp. 487–494.

[10] H. M. Park *et al*., "Design and Implementation of Data-Based Validation and Evaluation System for Combat System Engineering", *IEEE Access*, 2023, (Early Access).

[11] Volume of data/information created, captured, copied, and consumed worldwide from 2010 to 2020, with forecasts from 2021 to 2025 Available at: https://www.statista.com/statistics/871513/worldwide-data-created/.

[12] J. Martel *et al*., "Influence of electromagnetic fields on the circadian rhythm: Implications for human health and disease", *Biomedical Journal*, Vol. 46, Issue 1, 2023, pp 48–59.

[13] E. Mühlhofer *et al*., "A generalized natural hazard risk modelling framework for infrastructure failure cascades", *Elsevier: Reliability Engineering & System Safety*, Vol. 234, 2023.

[14] A. K. Dhami, "Study of electromagnetic radiation pollution in an Indian city", *Springer: Environmental Monitoring and Assessment*, Vol. 184, Issue: 11, 2012, pp. 6507–6512.

[15] WJ. Zhi, LF. Wang, and XJ. Hu, "Recent advances in the effects of microwave radiation on brains", *Military Medical Research*, Vol. 4, Issue: 29, 2017.

[16] R. Zhang et al., "Performance Analysis for MIMO-NOMA Systems with Transceivers and Group-Wise SIC", *in IEEE Transactions on Vehicular Technology*, (Early Access), 2023.

[17] B. M. Lee, "Exploring the Impact of Power Control Strategies for Enhanced IoT Connectivity in Massive MIMO", *in IEEE Internet of Things Journal*, (Early Access), 2023.

[18] H. Sharma *et.al.*, "PAPR Reduction Analysis by Implementing IFFT using Peak Windowing technique for Wireless Communication System", *3rd International Conference on Advance Computing and Innovative Technologies in Engineering (ICACITE)*, Greater Noida, India, 2023, pp. 819–823.

[19] Z. Cui, J. Chen and H. Zhao, "A Carbon Emission Reduction Method for Distribution Network with Data Centers", *First International Conference on Cyber-Energy Systems and Intelligent Energy (ICCSIE)*, Shenyang, China, 2023, pp. 1–4.

[20] K. Utkarsh, Ashish and P. Kumar, "Transmit power reduction in an IRS aided Wireless Communication System using DNN", *International Conference on Microwave, Optical, and Communication Engineering (ICMOCE)*, Bhubaneswar, India, 2023, pp. 1–5.

[21] S. Gupta, and A. Goel, "Chicken Swarm Optimization for PTS based PAPR Reduction in OFDM Systems", *Journal of Communications Software and Systems*, Vol. 16, No. 3, 2020, pp. 224–231.

[22] R. Abu-alhiga and H. Haas, "Subcarrier-index modulation OFDM", *IEEE 20th International Symposium on Personal, Indoor and Mobile Radio Communications*, Tokyo, Japan, 2009, pp. 177–181.

[23] X. Wang *et al*., "Constellation Reshaping Method for PAPR Reduction of SIM-OFDM based on SLM algorithm", *Asia Communications and Photonics Conference (ACP)*, Shanghai, China, 2021.

[24] X. Zou, S. Fan, H. Chen and Y. Xiao, "Efficient Signal Detection for MIMO-SIM-OFDM Systems", *IEEE 94th Vehicular Technology Conference (VTC2021-Fall)*, Norman, OK, USA, 2021, pp. 1–6.

[25] M. I. Kadir, H. Zhang, S. Chen and L. Hanzo, "Entropy Coding Aided Adaptive Subcarrier-Index Modulated OFDM" *IEEE Access*, Vol. 6, 2018, pp. 7739-7752.

[26] F. Khan et al., "A Novel Double-Sided Pulse Interval Modulation (DS-PIM) Aided SIM-OFDM for 6G Light Fidelity (LiFi) Networks", *Electronics*, Vol. 11, No. 21, 2022.

[27] D. Tsonev, S. Sinanovic and H. Haas, "Enhanced subcarrier index modulation (SIM) OFDM", *IEEE GLOBECOM Workshops (GC Wkshps)*, Houston, TX, USA, 2011, pp. 728–732.

[28] J. Seo *et al.*, "ESIM OFDM with Schmidl and Cox Algorithm Synchronizer in Rayleigh fading channel", *25th Asia-Pacific Conference on Communications (APCC)*, Ho Chi Minh City, Vietnam, 2019, pp. 267–270.

[29] A. Hilario-Tacuri, "On the Non-linearity Effects Over the Spectrum of ESIM-OFDM Based Systems", *42nd International Conference on Telecommunications and Signal Processing (TSP)*, Budapest, Hungary, 2019, pp. 278–281

[30] A. Hilario-Tacuri, "BER Analysis of ESIM-OFDM Systems Over Non-linearities With Memory", *IEEE XXVIII International Conference on Electronics, Electrical Engineering and Computing (INTERCON)*, Lima, Peru, 2021, pp. 1–4.

[31] A. N. Jabbar, S. J. Almuraab and A. A. Kadhim, "A New Analytical Model for SIM–OFDM Contradicts the Previously Claimed Features", *Journal of Communications Software and Systems*, Vol. 18, No. 3, 2022, pp. 228–235.

[32] E. O. Brigham, *The Fast Fourier Transform and Its Applications*, Prentice Hall, 1988.

[33] H. Gordon, *Discrete Probability*, Springer New York, 1997.

[34] M. Irfan and S. Aïssa, "On the Spectral Efficiency of Orthogonal Frequency-Division Multiplexing with Index Modulation", *IEEE Global Communications Conference (GLOBECOM)*, Abu Dhabi, United Arab Emirates, 2018, pp. 1–6.

[35] N. Ishikawa, S. Sugiura and L. Hanzo, "Subcarrier-Index Modulation Aided OFDM - Will It Work?", *IEEE Access*, Vol. 4, 2016, pp. 2580–2593.

[36] M. Pischella and D. L. Ruyet, *Digital Communications 2: Digital Modulations*, Wiley, 2015.

[37] M. K. Simon and M. S. Alouini, *Digital Communication Over Fading Channels: A Unified Approach to Performance Analysis*, Wiley, 2000.

[38] J. R. Barry, E. A. Lee and D. G. Messerschmitt, *Digital Communication*, 3rd Edition, Springer, 2003.

Ahmed N. Jabbar received the B. Sc. in Electronic and Communication Eng. in 1994 and M. Sc. In 1997 from Al-Nahrain University Baghdad, Iraq. He received the title of lecturer in 2009, associated professor in 2012 and professor title in 2018 from the University of Babylon. Currently, he is a professor and Ph. D. student in University of Babylon, College of Eng., Electronic and Communication Eng. Babylon city, Iraq since 2019. The field of interest is high speed communication systems, microwave system design and analysis, data mining, parallel hardware system design using FPGA and DSP for AI in communication systems.

Samir J. Almuraab was born in Hilla, Babylon, Iraq, in 9. Oct. 1959. He received the B.Sc. degree in Electrical Engineering/Electronics and Communications in 1981 from University of Sulaymaniyah, and the M.Sc. degree in Electrical Engineering/Electronics and Communications in 1986 from University of Baghdad and PhD. in communication Engineering at the Department of technical Education- Electrical Engineering, University of Technology. Currently, he works as a professor and Head of the Scientific Composition at the Electrical Department at the Faculty of Engineering, University of Babylon. His main interests are wireless communication, spread spectrum systems, digital video broadcasting (T, S &C), coding, wireless sensor network applications, bioinformatics, signal processing, healthcare system.

Abdulkareem Abdulrahman Kadhim was born in Baghdad, Iraq, in 1958. He received his B.Sc. degree in Electrical and Electronics Engineering in 1981 from MEC, Iraq, and M.Sc. and Ph.D. degrees from Loughborough University of Technology, UK, in 1984 and 1989, respectively, in Digital Communication Systems. He is an *IEEE* Senior Member and Member of ACM. Currently, he is a professor of Digital Communications in the College of Information Engineering, Al-Nahrain University, Iraq. He has published 66 papers in international and national journals and scientific conferences. He successfully supervised 11 Ph.D. dissertations and 62 M.Sc. theses. His research interests include modern error correction codes for next generation networks, detection of coded and modulated signals, low complexity decoders, millimetre wave channel modelling, network coding, software defined environments, and efficient routing for wireless sensor networks (WSNs) and IoT networks.